MODELING OF THE MICROSTRUCTURE EVOLUTION OF A STEEL BILLET DURING THE VARIOUS TYPES OF ROLLING IN RELIEF ROLLS

Dmitry Panin[1], Evgeniy Panin[1], Abdrakhman Naizabekov[2], Sergey Lezhnev[3], Aibol Esbolat[1], Nikita Lutchenko[4], Pavel Tsyba[1], Ivan Krupenkin[1], Denis Voroshilov[5]

[1]*Karaganda Industrial University, Temirtau, Kazakhstan, dimon802@mail.ru (D.P.); ye.panin@tttu.edu.kz (E.P.); esbolat.a@mail.ru (A.E.); tpl-work@mail.ru (P.T.); volkodav-007@mail.ru (I.K.)*
[2]*Science, Education and Staff Planning LLP Astana, Kazakhstan, naizabekov57@mail.ru (A.N.)*
[3]*Rudny Industrial University, Rudny Kazakhstan, sergey_legnev@mail.ru (S.L.)*
[4]*Nazarbayev University, Astana Kazakhstan, lutchenko1996@gmail.com (N.L.)*
[5]*Siberian Federal University, Krasnoyarsk Russia, d.s.voroshilov@gmail.com (D.V.)*

Received 23 January 2026
Accepted 30 April 2026
DOI: 10.59957/jctm.v61.i4.2026.18

ABSTRACT

The paper presents the results of microstructure evolution obtained by finite element modeling in the DEFORM program for various types of rolling in relief rolls: symmetric rolling, asymmetric rolling with an asymmetry coefficient of 1.5 due to the roll diameters of 200 and 300 mm, as well as single-drive rolling, in which one of the rolls is driven and the other roll is idling. After rolling in relief rolls, the billet undergoes two-stage leveling in smooth rolls. The presence of a single driven roll with the ability to adjust its rotational speed allows for a higher asymmetry coefficient. The microstructure evolution was evaluated using the Cellular Automata method, which allows for the assessment of changes in both the size and shape of the grains. It was found that using a billet with a heating temperature of 700°C is the most preferable option in all cases, as it eliminates the negative effect of static recrystallization, and the implementation of single-drive rolling allows for the highest degree of grain refinement.

Keywords: asymmetric rolling, modeling, microstructure, Cellular Automata, FEM.

INTRODUCTION

For decades, asymmetric rolling has been a promising high-tech method for producing high-quality metal products in the form of hot-rolled sheets and thick plates. During this process, additional shear deformation flows are implemented in the deformed material [1]. The most common types of asymmetric rolling include kinematic rolling (different roll speeds), geometric rolling (different roll diameters), and the use of a non-driven (idling) roll, as shown in Fig. 1 [2, 3]. During asymmetric thin-sheet rolling, additional shear deformations occur, which, when combined with compression deformations, can effectively reduce grain size.

For each of these options, various technological schemes for implementing asymmetric rolling in practice have been developed, including the availability of auxiliary devices and mechanisms for inclusion in a continuous rolling line [4 - 7]. A number of studies have focused on the asymmetric rolling of bimetallic billets, which can consist of either entirely non-ferrous metals or a combination of non-ferrous metals and steels [8 - 10]. As a result of the asymmetric rolling process, these billets developed an ultrafine-grained structure with improved mechanical properties. Additionally, the review highlights that the key feature of asymmetric rolling is the uneven processing of the billet's height, resulting in a gradient of properties across the cross-

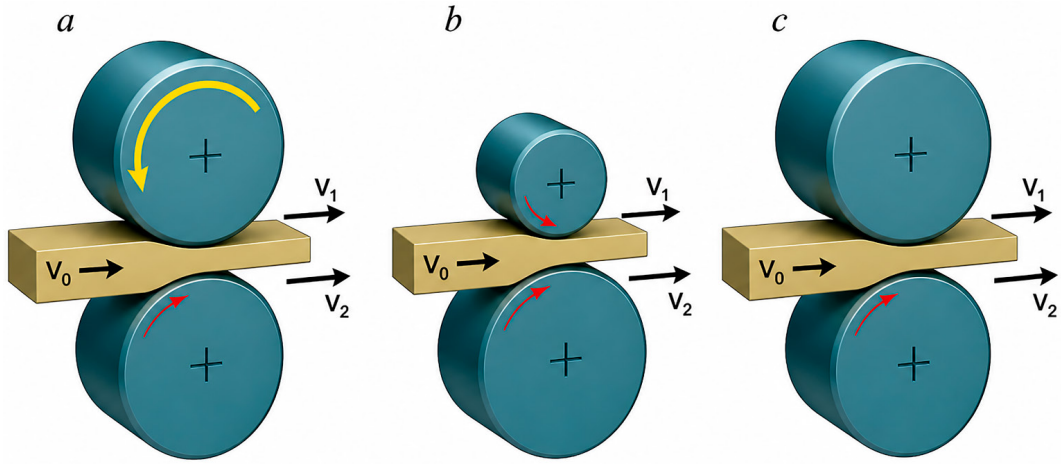

Fig. 1. Variants of asymmetric rolling: (a) - in rolls with different circumferential speeds; (b) - in rolls of different diameters; (c) - with one non-driven roll.

section [11].

The technology of rolling thick sheet metal has been investigated, which has solved the problem of producing high-quality thick sheet metal without significantly altering the initial dimensions of the billet [12, 13]. To achieve this, two variants of rolls with a relief profile in the form of annular grooves have been developed. It has been determined that the most optimal design is the relief rolls with a varying ratio of the protrusion to the depression. Additionally, a method of geometric asymmetry using relief rolls of different diameters has been implemented to achieve a high level of asymmetry (Fig. 2).

The essence of the proposed solution was to use relief rolls with a profile in the form of trapezoidal protrusions and depressions during asymmetric rolling [14, 15]. The use of such rolls allows for additional shear deformation during rolling, not only in the longitudinal direction (as in asymmetric rolling with smooth rolls), but also in the transverse direction. Additionally, even with a high level of asymmetry, the workpiece did not bend significantly after exiting the deformation zone of the relief rolls, maintaining its horizontal trajectory. This effect was achieved due to the resulting relief profile of the workpiece, where the protrusions and depressions acted as stiffeners. This method proved to be highly effective in terms of metal cross-section development and improving the mechanical properties of aluminum and copper thick-sheet workpieces.

It is important to note that both the most common

Fig. 2. Cage with relief rolls of different diameters.

methods of implementing asymmetric rolling (geometric and kinematic) have their own technological drawbacks. For example, implementing geometric asymmetry for a wide range of thick-sheet products requires the production of a large number of rolls with different diameters. Additionally, it is often impossible to achieve a high asymmetry coefficient with geometric asymmetry due to the limited range of roll diameters imposed by the structural dimensions of the mill stand. On the other hand, implementing kinematic asymmetry does not have

explicit limitations on the asymmetry coefficient and depends on the ability to adjust the speeds of the electric motors. However, this method of asymmetry requires a significant redesign of the rolling mill to provide individual roll drives with the ability to adjust the circumferential speeds of each working roll separately.

An alternative solution to these disadvantages is to use a rolling mill with a single driven roll, which can further improve the processability of high-quality metal products such as hot-rolled sheets and thick plates [16]. In this case, the disadvantages listed above are eliminated, as the presence of rolls with different diameters is not a prerequisite for creating asymmetry, and their presence can actually enhance the asymmetry effect. The use of a single driven roll with the ability to adjust its rotational speed allows for a higher degree of asymmetry, as the second roll is non-driven (idle) and only rotates due to the active friction forces between the roll and the workpiece. In this case, it is sufficient to physically disconnect one roll from the drive system, which does not require significant modifications to the rolling mill.

The purpose of this study was to simulate the microstructure evolution of a steel workpiece during various types of rolling in relief rolls to assess their effectiveness in terms of metal processing and grain refinement.

EXPERIMENTAL

In this work, it was decided to conduct all theoretical studies in the DEFORM program, as the most actively developing product in the field of modeling of metal forming processes. In order to fully analyze the microstructure evolution of a steel billet during single-drive rolling in relief rolls, it was decided to conduct a multifactorial simulation with simultaneous variation of technological parameters. In this case, the parameters that could be further implemented in real laboratory conditions were selected as the variables. It was decided to deform the billet on a mill at Karaganda Industrial University, where experiments on deforming aluminum and copper billets of similar thickness were previously successfully conducted [15]. The laboratory mill allows for rolling in both symmetrical mode (both rolls have a diameter of 200 mm) and asymmetrical mode with an asymmetry coefficient of 1.5 (the upper roll has a diameter of 200 mm, and the lower roll has a diameter of 300 mm).

The first technological parameter was the temperature of the billet, which has a significant impact on both the stress state during deformation and the recrystallization process. Since this study uses a common AISI 1015 steel, the following temperature values were selected: 1100°C (hot rolling with static recrystallization) and 700°C (hot rolling without activating the static recrystallization mechanism).

The second technological parameter is related to the kinematics of the rolling process. It was decided to conduct a detailed study of the influence of the rotation speed of the relief rolls. To achieve this, three rolling cases were simulated:

1) symmetrical rolling in relief rolls (both rolls rotate at a speed of 60 rpm);

2) asymmetrical rolling in relief rolls (asymmetry coefficient of 1.5);

3) single-drive rolling in relief rolls (the upper relief roll is disconnected from the spindle, making it idle and rotating due to friction when in contact with the billet).

The design of the relief surface of the rolls is shown in Fig. 3.

The roll barrel length was 400 mm. The diameter of the smooth rollers for aligning the workpiece was 200 mm. The workpiece was a rectangular sheet with a cross-section of 10 × 300 mm and a length of 350 mm. It was decided to simulate rolling with a symmetry plane

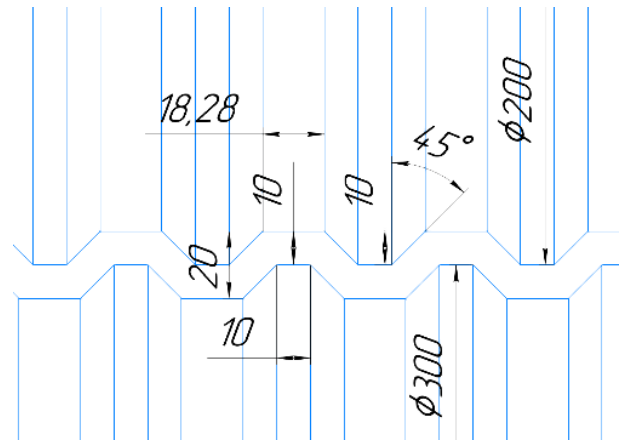

Fig. 3. Design of relief rolls for rolling a 10 mm thick workpiece.

in the width direction, i.e., the width of the workpiece was 200 mm in the models, which was mirrored. AISI 1015 steel was chosen as the workpiece material. The following technological parameters were used in the computer simulation of the process:

- workpiece material was completely isotropic;
- rolling was performed at an ambient temperature of 20°C;
- temperature of the workpiece before rolling was 1100°C and 700°C;
- heat transfer coefficient between the workpiece and the tool was 5000 W m^{-2} $°C^{-1}$;
- heat transfer coefficient between the workpiece and the environment was 0.002 W m^{-2} $°C^{-1}$;
- to create the most severe conditions of grip, the coefficient of friction at the metal-roll contact was assumed to be 0.7 (which corresponds to a rough surface with notches and a high level of roughness).

Adaptive solver settings were used to create a finite element mesh. Instead of using a fixed number of finite elements, the minimum size of a tetrahedral element was set to 1.5 mm. This ensures that there are at least 6 elements in the thickness of the workpiece, regardless of the mesh reconfiguration. This number of elements in the thickness is sufficient to accurately represent the shape changes. Since the design of the gap in the embossed rolls implies a maximum amplitude of the workpiece equal to twice its thickness, the gaps for alignment in the second and third passes were set to 25 % and 50 %, respectively. This means that for a workpiece with a thickness of 10 mm, the gap in the second pass was set to 15 mm, and in the third pass, it was set to 10 mm.

The JMAK method is not capable of capturing changes in the shape of the initial grain, but the Cellular Automata method can. However, this method has its own limitation, as it only allows for the microstructure study at predetermined points. Given these limitations, it was decided to use the Cellular Automata method in this study to obtain data on both the size and shape of the grains. To use this method, it is necessary to determine the points on the workpiece where the structure will be modeled. Early, during study the stress-strain parameters, it was found that the level of strain increases most significantly at the contact points with the embossed rolls [14]. However, there is a significant difference in the impact on the workpiece from the rolls in the asymmetric and single-drive cases. Therefore, it was decided to use the scheme (Fig. 4). In the two sections that encompass the relief rolls, three points are defined on both horizontal surfaces and in the center. In the symmetric models, only one section with three points was considered due to the identical impact on the workpiece from the rolls.

The cellular automata algorithm uses the calculated data of the stress-strain state, the strain rate, and the temperature from the ready-made model in DEFORM, and complements it with the data of the physical and chemical properties and their behavior for a given material and its structure. According to the Yada algorithm, it calculates the parameters of the processes of static and dynamic recrystallization, which affect the change in grain size, and the imposition of the deformation-velocity scheme affects the change in grain shape [17].

The algorithm used employs a large number of model coefficients, which are individual for different materials and deformation modes. These coefficients are discussed in detail in the work of professor Lenard, where a large number of values of these coefficients are presented for various grades of steel and alloys, depending on the types of deformation and heat treatments [18]. Below is a ready-made Yada algorithm with coefficients for

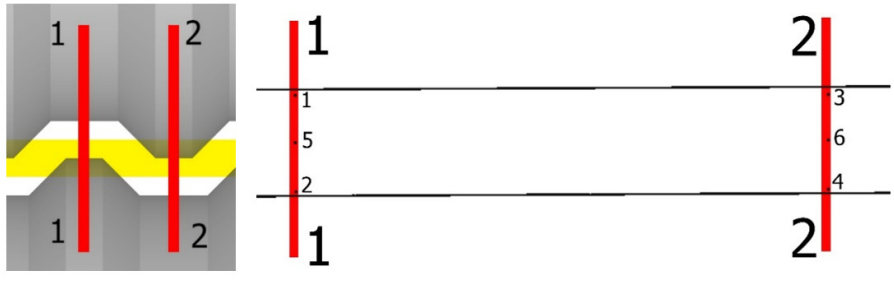

Fig. 4. Cross-sections and points for microstructure analysis [14].

low-carbon steel subjected to hot rolling.

During deformation, two types of recrystallization occur: static and dynamic, which affect the change in the initial grain size. The calculation of dynamic recrystallization is part of the model that deals with the processes in the deformation zone. It begins when the equivalent strain ε exceeds the critical strain ε_k. The main parameter of this model is the Zenner-Hollmon parameter (Eq. (1)):

$$Z = \dot{\varepsilon} \cdot \exp\left(\frac{312000}{RT}\right) \quad (1)$$

where $\dot{\varepsilon}$ - strain rate, s^{-1}; R - gas constant (8,3144 $J \cdot mol^{-1} \cdot K^{-1}$); T - deformation temperature, K.

Critical strain for the start of dynamic recrystallization (Eq. (2)):

$$\varepsilon_k = [4.9 \cdot 10^{-4} \cdot D_0^{0.5} \cdot Z^{0.15}] \cdot 1.23 \quad (2)$$

where D_0 - initial grain size, μm; Z - Zenner-Hollmon parameter.

Strain at 50 % dynamic recrystallization (Eq. (3)):

$$\varepsilon_{50} = [1.144 \cdot 10^{-3} D_0^{0.28} \cdot \dot{\varepsilon}^{0.05} \cdot \exp(51880 / RT)] \quad (3)$$

Dynamically recrystallized part (Eq. (4)):

$$X_{Dyn} = 1 - \exp[-0.4 \cdot ((\varepsilon - \varepsilon_k)/ \varepsilon_{50})^{1.5}) \quad (4)$$

Grain size after dynamic recrystallization, μm (Eq. (5)):

$$D_{Dyn} = 2.26 \cdot 10^4 \cdot Z^{-0.27} \quad (5)$$

The calculation of static recrystallization is a part of the model when the studied segment of the workpiece is not in the deformation zone. The calculation is carried out until static recrystallization is interrupted by the deformation stage or phase transition.

The amount of strain after the start of static recrystallization (Eq. (6)):

$$\varepsilon_m = 0.8 \cdot (\varepsilon_k + \varepsilon_{50} \cdot \{1 - \exp[-(\varepsilon - \varepsilon_k)/ \varepsilon_{50}]\}) \quad (6)$$

Time for 50 % static recrystallization, s (Eq. (7)):

$$t_{50} = 5 \cdot 10^{-21} \cdot \varepsilon^{-4} \cdot D_0^2 \cdot \exp(\frac{39711}{T}) \cdot \dot{\varepsilon}^{-0.28} \quad (7)$$

Time of the beginning and end of static recrystallization, s (Eq. (8) and Eq. (9)):

$$t_{05} = 0.01 \cdot t_{50} \quad (8)$$

$$t_{95} = 1.9 \cdot t_{50} \quad (9)$$

Pause time for temperature adjustment, s:

$$t_{P\_kor} = \sum \left\{ d_{Ti} \cdot \exp\left[-\left(\frac{330}{R \cdot T} \right) \right] \right\} \quad (10)$$

where d_{Ti} - the amount of time increment, s.

Statically recrystallized part:

$$X_{Stat} = 1 - \exp[-0.639 \cdot (t_{P\_kor}/t_{50})^{1.7}] \quad (11)$$

Grain size after static recrystallization, μm:

$$D_{Stat} = [6.2 \cdot \varepsilon^{55.7} \cdot D_0^{0.653} \cdot Z^{0.5}] + 0.35 \quad (12)$$

Grain size after both recrystallizations:

$$D = X_{Dyn} D_{Dyn} + (1 - X_{Dyn}) X_{Stat} D_{Stat} + \left[1 - X_{Dyn} - \left(1 - X_{Dyn} \right) X_{Stat} \right] D_0 \quad (13)$$

.

With long pauses between deformation stages, grain growth begins immediately after static and dynamic recrystallization ends, when (X_{Dyn} + X_{Stat}) > 95 % и (t_{P_kor} - t_{95}) > 0. The new value mKG of the grain size in μm is calculated using the Eq. (14):

$$mKG^{0.81} - D^{0.81} = 4.3 \cdot (t_{P\_kor} - t_{95}) \cdot \exp[-330000/(RT)] \quad (14)$$

To display the simulation results, the window settings were set to square, with dimensions of 150 μm by 150 μm. The initial metal structure in the annealed state was set to an equiaxed grain arrangement with an average size of 40 μm (Fig. 5).

Before modeling, it is necessary to determine the direction of view for studying the microstructure. For a complete picture, the transverse and longitudinal directions are considered. However, previous experimental studies [15] have shown that the grain size is almost identical in both directions, while the change from an equiaxed to an elongated grain shape is observed only in the longitudinal direction. Therefore, it was decided to consider only the longitudinal direction.

Additionally, the effect of static recrystallization

should be taken into account during the calculation. For the AISI 1015 steel used, the process of static recrystallization begins at approximately 730°C. With this value, models with a temperature of 700°C will be calculated without considering static recrystallization, while models with a temperature of 1100°C will undergo intensive static recrystallization.

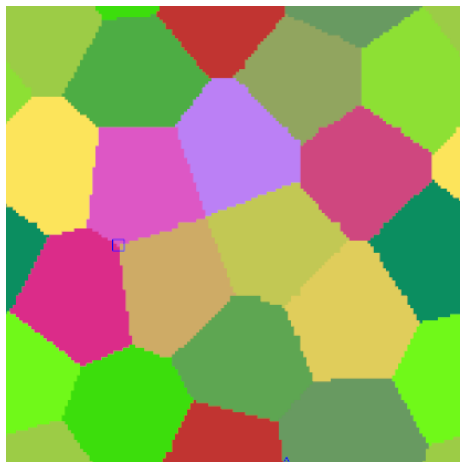

Fig. 5. Initial microstructure.

RESULTS AND DISCUSSION

Fig. 6 - 10 show the results of microstructure evolution modeling for a 10 mm thick workpiece. Below are the explanations for the selected points 1 - 6:

- point 1 is at the depression of the upper relief roll (200 mm);
- point 2 is at the protrusion of the lower relief roll (300 mm);
- point 3 is at the protrusion of the upper relief roll (200 mm);
- point 4 is at the depression of the lower relief roll (300 mm);
- point 5 is the central zone of section 1-1;
- point 6 is the central zone of section 2-2.

The values of the average grain size during symmetrical rolling for a 10 mm thick billet are shown in Table 1.

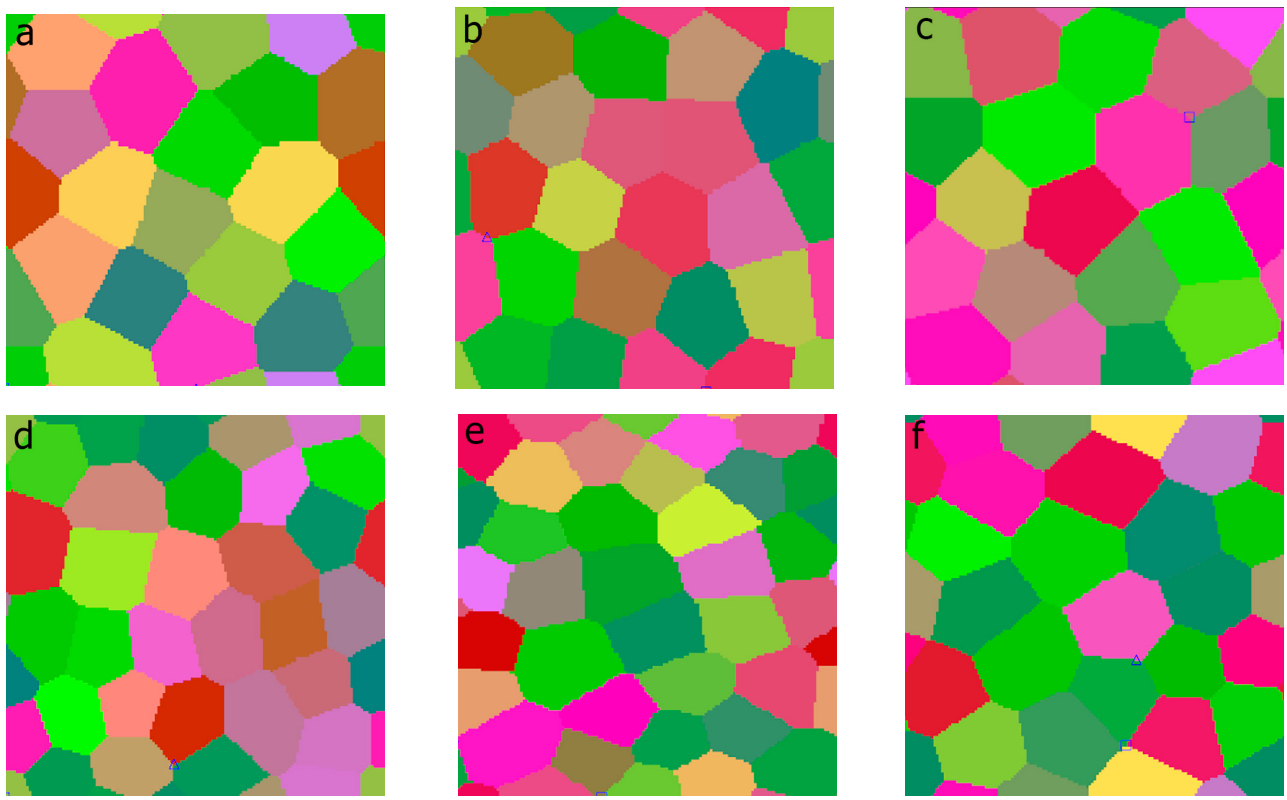

Fig. 6. Microstructure in the longitudinal section during symmetrical rolling: (a) - point 1 at 1100°C; (b) - point 2 at 1100°C; (c) - point 5 at 1100°C; (d) - point 1 at 700°C; (e) - point 2 at 700°C; (f) - point 5 at 700°C.

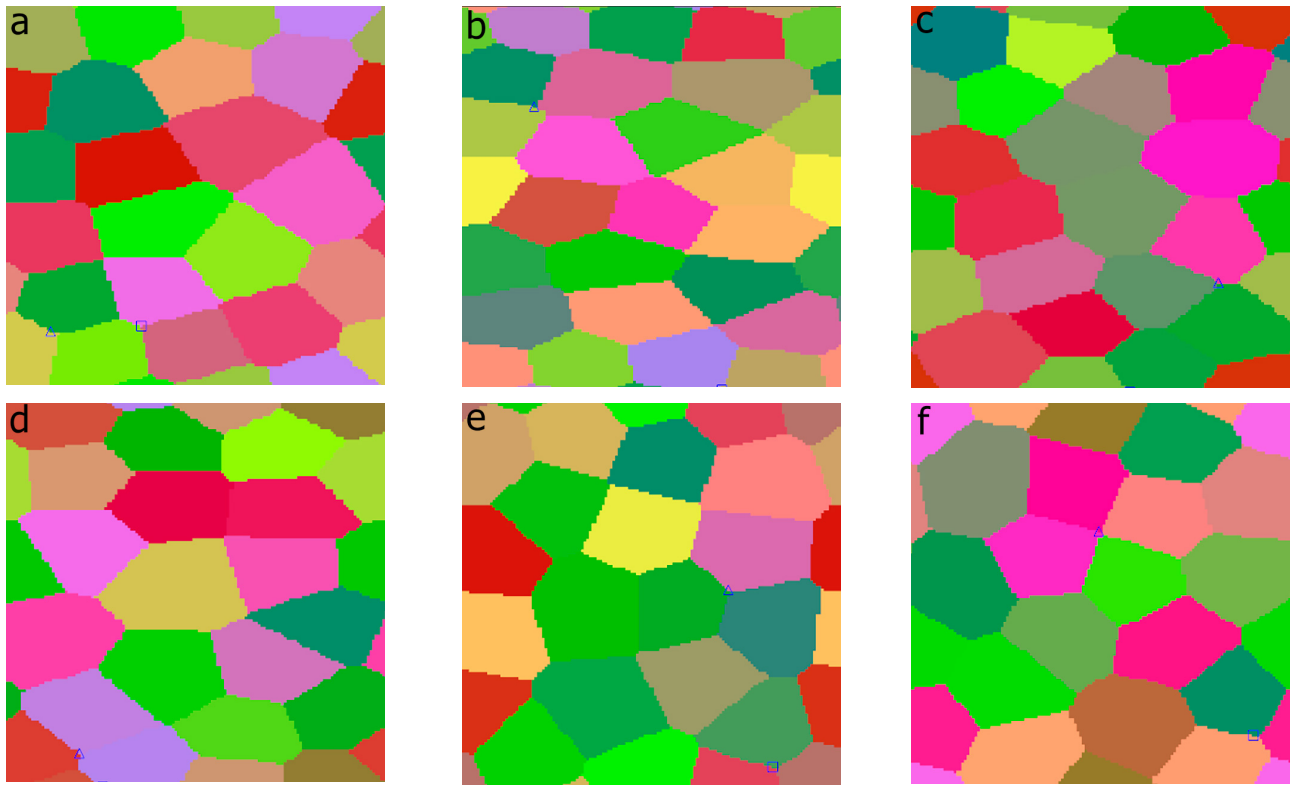

Fig. 7. Microstructure in the longitudinal section during asymmetric rolling at 1100°C: (a) - point 1; (b) - point 2; (c) - point 3; (d) - point 4; (e) - point 5; (f) - point 6.

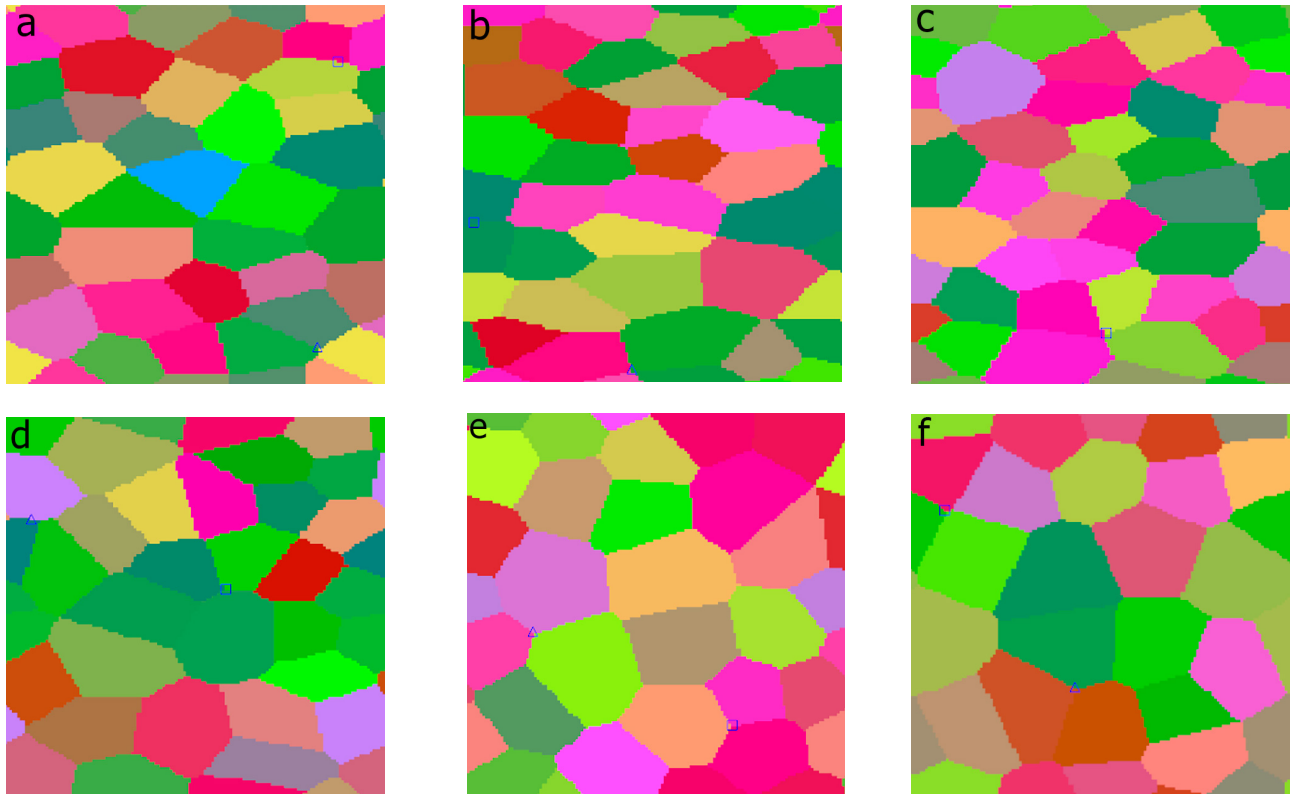

Fig. 8. Microstructure in the longitudinal section during asymmetric rolling at 700°C: (a) - point 1; (b) - point 2; (c) - point 3; (d) - point 4; (e) - point 5; (f) - point 6.

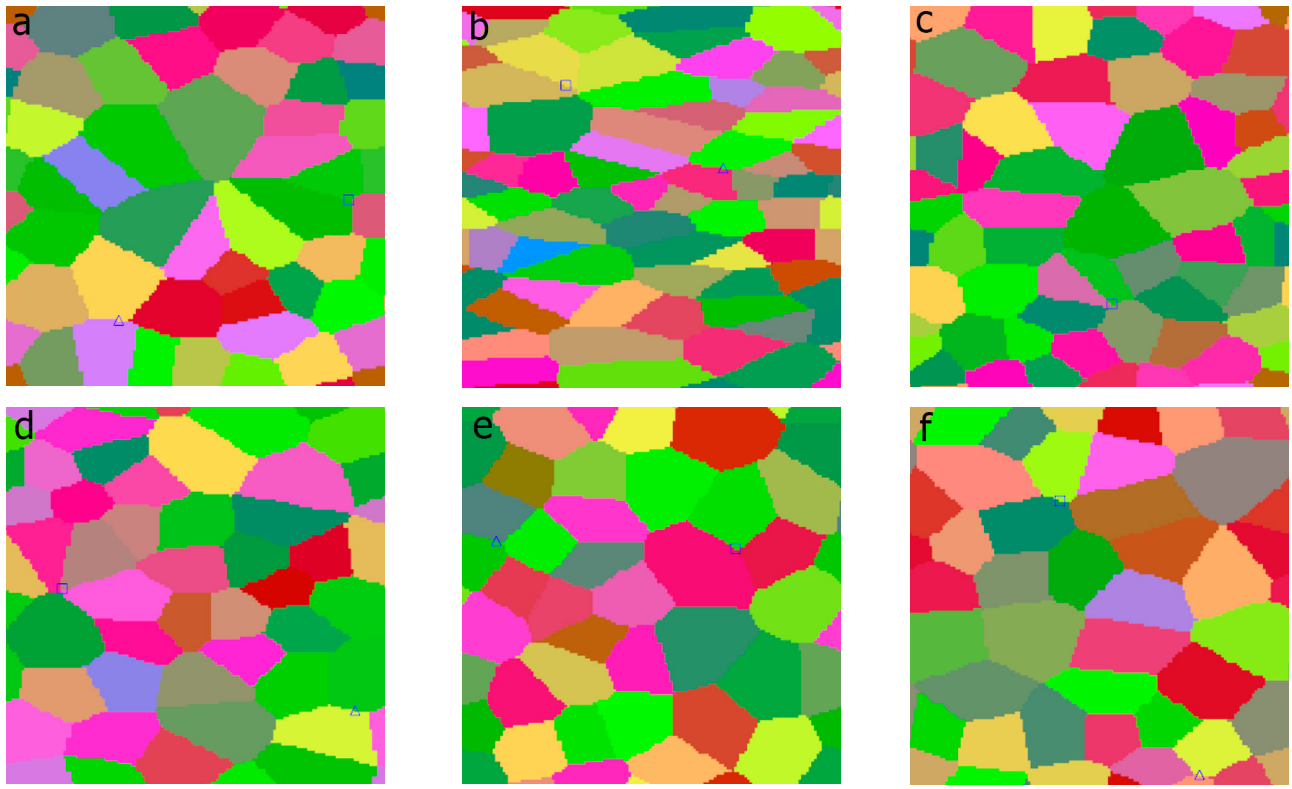

Fig. 9. Microstructure in the longitudinal section during single-drive rolling at 1100°C: (a) - point 1; (b) - point 2; (c) - point 3; (d) - point 4; (e) - point 5; (f) - point 6.

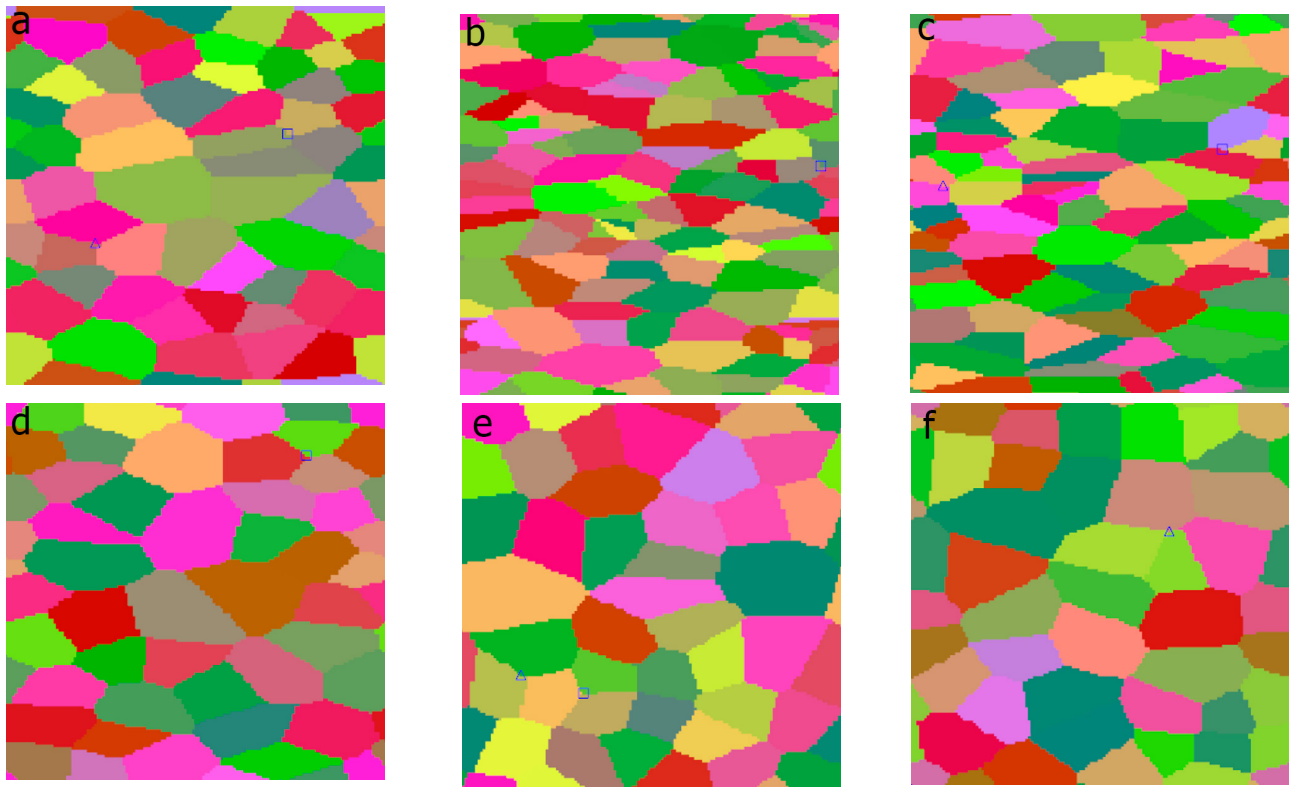

Fig. 10. Microstructure in the longitudinal section during single-drive rolling at 700°C: (a) - point 1; (b) - point 2; (c) - point 3; (d) - point 4; (e) - point 5; (f) - point 6.

Table 1. Average grain size for a 10 mm thick billet with symmetrical rolling, μm.

Rolling model	Point 1	Point 2	Point 3	Point 4	Point 5	Point 6
Symmetrical, 1100°C	37	35	-	-	38	-
Symmetrical, 700°C	30	29	-	-	34	-

Table 2. Average grain size for a 10 mm thick workpiece during asymmetric rolling, μm.

Rolling model	Point 1	Point 2	Point 3	Point 4	Point 5	Point 6
Asymmetric, 1100°C	36	34	35	36	38	38
Asymmetric, 700°C	29	28	28	30	34	34

Table 3. Average grain size for a 10 mm thick workpiece during single-drive rolling, μm.

Rolling model	Point 1	Point 2	Point 3	Point 4	Point 5	Point 6
Single-drive, 1100°C	25	21	23	26	28	28
Single-drive, 700°C	22	16	18	25	26	26

When considering the results of symmetric rolling, three features can be noted:

1) at a lower temperature, the overall level of grain refinement is more intense due to the absence of the static recrystallization effect;

2) only in the model at 700°C at point 2 (on contact with the protrusion), there is a slight elongation of the grains, while in other cases, the grains remain equiaxed;

3) the surface layers experience greater refinement than the central zone.

The average grain size values for asymmetric rolling for a 10 mm thick workpiece are presented in Table 2.

When considering the results of asymmetric rolling, the following features can be noted:

1) the effect of more intensive grain refinement at lower temperatures is present;

2) grain elongation is observed at both temperatures, but in the 700°C model, grain elongation is more pronounced due to the absence of static recrystallization. In each section 1-1 and 2-2 (Fig. 4), grain elongation is more pronounced at the contact with the roll protrusion;

3) in the 700°C model, all layers undergo greater refinement than in the corresponding symmetric rolling model due to the additional effect of asymmetry. In the 1100°C model, this effect is almost invisible due to the negative influence of static recrystallization.

The average grain size values for single-drive rolling for a 10 mm thick workpiece are presented in Table 3.

When considering the results of single-drive rolling, the following features can be noted:

1) there is a grain refinement effect at lower temperatures, which is more pronounced than in any other model;

2) the grain elongation pattern is similar to that observed during asymmetric rolling (the elongation is more pronounced in the 700°C model). However, the level of elongation is even more pronounced, especially at the contact with the roll protrusions, which indicates a higher level of asymmetry due to the presence of an idle roll;

3) in the 700°C model, the surface layers exhibit a refinement level of 55 - 60 % of the initial grain size, while the refinement in the central layers is significantly lower. This is a result of the high level of asymmetry and the absence of static recrystallization.

CONCLUSIONS

The paper proposed a new method of asymmetric rolling, in which the first pass is performed in relief rolls with an asymmetry factor (geometric or kinematic). In this method, only one roll is driven, while the other roll is idled. After rolling in the relief rolls, the workpiece undergoes an alignment process in smooth rolls. The presence of a single driven roll with the ability to adjust the rotational speed of the driven roll allows for a higher asymmetry factor. The evaluation of the microstructure evolution showed that using a workpiece with a heating temperature of 700°C is the most preferable option, as it eliminates the negative effect of static recrystallization. Additionally, at this temperature, the implementation of a single-drive deformation method allows for the highest degree of grain refinement. Based on these findings, the single-drive rolling method can be considered the most effective.

Acknowledgements

This research was funded by the Science Committee of the Ministry of Science and Higher Education of the Republic of Kazakhstan (Grant № AP26199255).

Authors' contributions

D.P.: investigation, writing - original draft; E.P.: investigation, funding acquisition, project administration; A.N.: methodology; S.L.: conceptualization, methodology, investigation; A.E.: writing - review & editing; N.L.: validation, data curation, software; P.T.: visualization, investigation; I.K.: resources; D.V.: formal analysis.

REFERENCES

1. D. Pustovoytov, A. Pesin, P. Tandon, Asymmetric (Hot, warm, cold, cryo) rolling of light alloys: A review, Metals, 11, 2021, 956.
2. Y.H. Ji, J.J. Park, W.J. Kim, Finite element analysis of severe deformation in Mg-3Al-1Zn sheets through differential-speed rolling with a high speed ratio, Mater. Sci. Eng., A, 454, 2007, 570-574.
3. Y.H. Ji, J.J. Park, Development of severe plastic deformation by various asymmetric rolling processes, Mater. Sci. Eng., A, 499, 2009, 14-17.
4. V.M. Salganik, A.M. Pesin, Asymmetric Thin-Sheet Rolling: Development of Theory, Technology and New Solutions, Moscow, MISIS, 1997.
5. G. Vincze, F. Simões, M. Butuc, Asymmetrical rolling of aluminum alloys and steels: A review, Metals, 10, 2020, 1126.
6. S.M. Belsky, Improving the technology of forming strips and sheets based on the development of the theory of symmetric and asymmetric hot rolling, Lipetsk: LSTU, 2009.
7. H.L. Yu, C. Lu, A.K. Tieu, H.J. Li, A. Godbole, S.H. Zhang, Special rolling techniques for improvement of mechanical properties of ultrafine-grained metal sheets: a review, Adv. Eng. Mater., 18, 2016, 754-769.
8. D. Chang, P. Wang, Y. Zhao, Effects of asymmetry and annealing on interfacial microstructure and mechanical properties of Cu/Al laminated composite fabricated by asymmetrical roll bonding, J. Alloys Compd., 815, 2020, 152453.
9. X. Li, G. Zu, M. Ding, Y. Mu, P. Wang, Interfacial microstructure and mechanical properties of Cu/Al clad sheet fabricated by asymmetrical roll bonding and annealing, Mater. Sci. Eng., A, 529, 2011, 485-491
10. S.H. Zhang, D.W. Zhao, C.R. Gao, G.D. Wang, Analysis of asymmetrical sheet rolling by slab method, Int. J. Mech. Sci., 65, 2012, 168-176.
11. E.X. Cui, T.J. Chen, Y.F. Shen, N. Jia, Z.D. Wang, Z.J. Fan, Superior combination of strength and ductility in Fe-20Mn-0.6C steel processed by asymmetrical rolling, Mater. Today Commun., 40, 2024, 110064.
12. A. Naizabekov, S. Lezhnev, E. Panin, I. Mazur, Alternating Sign Rolling Technology in Grooved Rolls for Nonferrous Metal Plate Billets, Metallurgist, 61, 2017, 406-413.
13. A. Naizabekov, S. Lezhnev, T. Koinov, I. Mazur, E. Panin, Research and Development of Technology for Rolling of High-Quality Plates of Non-Ferrous Metals and Alloys in Relief Rolls, J. Chem. Technol. Metall., 51, 2016, 363-370.
14. E. Panin, A. Esbolat, A. Arbuz, D. Kuis, A. Naizabekov, S. Lezhnev, A. Yerzhanov, I. Krupenkin, A. Tolkushkin, A. Kawalek, P. Tsyba, Investigation of the Efficiency of Roll Profiles and Technological Schemes of Deformation of Asymmetric Rolling in Relief Rolls of C11000 Copper Alloy by FEM Simulation, Modell. Simul. Eng., 2024, 2024, 2486940.
15. S. Lezhnev, A. Naizabekov, A. Esbolat, A. Rakovets, E. Panin, D. Kuis, P. Tsyba, D. Panin, S. Kuzmin, Effect of asymmetric rolling in relief rolls on the microstructure evolution and mechanical properties of aluminum and copper workpieces, Results Eng., 26, 2025, 105195.
16. W. Baba, M. Miyake, J. Yanagimoto, Warping behavior of thin strip with single-drive rolling, Key Eng. Mater., 725, 2017, 537-541.
17. H. Yada, N. Matsuzu, K. Nakajima, K. Watanabe and H. Tokita, Strength and Structural Changes under High Strain-rate Hot Deformation of C Steels, Trans. ISIJ, 23, 1983, 100-109.
18. J.G. Lenard, M. Pietrzyk, L. Cser, Mathematical and Physical Simulation of the Properties of Hot Rolled Products, Amsterdam, Elsevier, 2005.